3D Human Shapes Correspondence using the Principal Curvature Fields on a Local Surface Parametrization

Ilhem Sboui, Majdi Jribi and Faouzi Ghorbel
CRISTAL Laboratory, GRIFT Research Group, National School of Computer Sciences, La Manouba University, La Mannouba, Tunisia
ilhem.sboui@gmail.com, majdi.jribi@ensi.rnu.tn, faouzi.ghorbel@ensi.rnu.tn

Keywords: 3D Human Shapes, Correspondence, Darcyan Coordinates System, Principal Curvatures, Symmetry.

Abstract: In this paper, we address the problem of the correspondence between 3D non-rigid human shapes. We propose a local surface description around the 3D human body extremities. It is based on the mean of principal curvature fields values on the intrinsic Darcyan parametrization constructed around these points. The similarity between the resulting descriptors is, then, measured in the sense of the L_2 distance. Experiments on a several human objects from the TOSCA dataset confirm the accuracy of the proposed approach.

1 INTRODUCTION

Non-rigid three-dimensional shapes matching has been an active research topic in computer vision over the last years. It is a key task in many applications such as space-time reconstruction, motion tracking and recognition, shape retrieval and videos indexing. The goal of non rigid shape matching is to find a map $f : S \rightarrow T$ between points on one surface S to their equivalent points on a second surface T.
The problem of establishing a correspondence between non-rigid shapes remains challenging and particularly tough since the correspondence involves surfaces representing different poses of an articulated objects and generally highly deformed surfaces.
In this context, several methods have been proposed for finding a correspondence between non-rigid 3D shapes in the state-of-the-art. A detailed survey on 3D shapes matching methods was proposed by (Van Kaick et al., 2010). Two categories of 3D non-rigid correspondence can be distinguished according to the resolution of the matched points: sparse and dense. Various approaches have addressed the sparse correspondence which aims to map a small set of points on a given surface. The most common ones consist on extracting local shape descriptors at a set of feature points. (Zhang et al., 2008) proposed a method which is robust to the symmetry problem and consists on deforming a given shape to have alignment between feature points and then minimizing resulting distortion. Later, (Zheng et al., 2013) proposed a shape descriptor based on iso-lines of harmonic fields between shape extremal points to establish a correspondence. Then, they, demonstrated the effectiveness of their descriptor to intrinsic reflectional symmetry. (Yaron and Thomas, 2009) proposed a method for only nearly-isometric surfaces using the Mobius transform. A descriptor based on fuzzy geodesics to find correspondences between sparse sets of points on shapes differing by extreme deformations was presented by (Sun et al., 2010). On the other hand, (Ovsjanikov et al., 2010) proposed an approach which relies on matching feature points in a space of a heat kernel for a given point on a surface and then the correspondence is obtained by searching the most similar heat kernel maps . Moreover, (Yusuf Sahillioğlu, 2014) proposed an algorithm relying on the dynamic programming to match shape extremities which was unable to completely alleviate the symmetrical flip problem.
One of the alternatives centered around the notion of minimum distortion correspondence is the method of (Bronstein et al., 2006). They introduced the generalized multidimensional scaling (GMDS) which allows finding the minimum distortion embedding of one surface onto another using an approximation to the Gromov-Hausdorff distance.
Various prominent methods in the literature seek to find dense correspondence between 3D non-rigid shapes. One of the notable approaches is proposed by (Kim et al., 2011) consisting on combining multiple low-dimensional intrinsic maps to produce a blended map. They, then, associated confidence and consistency weights to each map and find the best blending to establish a final correspondence. An other alternative, introduced also by (Bronstein et al., 2009) was

Sboui I., Jribi M. and Ghorbel F.
3D Human Shapes Correspondence using the Principal Curvature Fields on a Local Surface Parametrization.
DOI: 10.5220/0006266606310636
In *Proceedings of the 12th International Joint Conference on Computer Vision, Imaging and Computer Graphics Theory and Applications (VISIGRAPP 2017)*, pages 631-636
ISBN: 978-989-758-225-7

based on the diffusion distance instead of the geodesic one in the GromovHausdorff framework. Some attempts to find dense correspondence based on embedding the shapes onto a spectral domain like the approach of (Jiang et al., 2013) using a non-rigid variant of the ICP (Iterative Closest Point) algorithm and (Aalo et al., 2013) who proposed a spectral formulation for the generalized multidimensional scaling method denoted as spectral GMDS.
Within this context, (Taylor et al., 2012) focused on matching human shapes in various poses using an efficient learned regression function for the articulated shapes correspondences.
Very recently, (Wei et al., 2015) developed a new deep learning approach using a convolutional neural network architecture for finding dense correspondences between human bodies.
In this paper, we propose a novel approach to find a sparse correspondence between deformed shapes of type 3D human body. Our proposal consists on an intrinsic local description of the human surfaces extremities. It is based on the construction of a local discrete representation known by Darcyan Coordinates System. Then, principal curvatures field are computed for each discrete representation around the extracted extremities. Matched points are obtained by measuring the similarity between their correspondent local representations in the sense of the L_2 distance.
Thus, this paper will be structured as follows: In the second section, we describe the proposed descriptor construction process. For the next section, we represent our 3D human bodies correspondence approach. The fourth section is devoted to the experimental results on 3D human objects from the TOSCA dataset and our proposed solution to handle the problem of the symmetry.

2 HUMAN SHAPES CORRESPONDENCE

We intend to establish a sparse correspondence between 3D human body objects with different non rigid deformations. We propose to make a correspondence between these shapes extremities since they give a good description of human body structure. The proposed approach is based on an intrinsic description of the extreme points neighborhood using the darcyan representation and the principal curvature field. We present, in this section, all the steps of the construction of the novel local description around the extremities points.

2.1 Extremities Extraction

In this section, we intend to extract extremities over the human body shapes applying the robust approach proposed by (Julien et al., 2006) which results a set of interest points invariant to the human pose. This approach is described below:
Let x_1 and x_2 be the farthest vertices on a surface mesh M in the sense of the geodesic distance. We denote by $g_{dist}(x,y)$ the geodesic distance between x and y two vertices on M.
We consider g_1 and g_2 two scalar functions associated to each vertex x of M. g_1 and g_2 are defined as follow:

$$g_1 = g_{dist}(x,x_1) \text{ and } g_2 = g_{dist}(x,x_2)$$

We denote by E_1 and E_2 the sets of the local extrema of, respectively, g_1 and g_2 . The set of extremities, denoted by E, is defined by the intersection of E_1 and E_2:

$$E = E_1 \bigcap E_1$$

Figure 1 illustrates the resulting extreme points on 3D human surfaces.

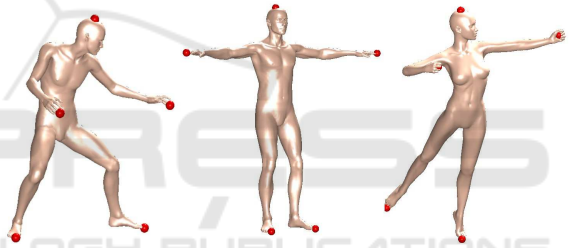

Figure 1: 3D human shapes extremeties.

2.2 Darcyan Coordinates System Representation

After the extraction of the extreme points, local description around these points must be performed in order to ensure the good correspondence between different shapes. But, for the same 3D object, different meshes may exist. In fact, each mesh depends on its initial parametrization. For this reason, we propose to use the well known Darcyan Coordinates System, introduced by D'Arcy Thompson (Thompson, 1917). Such parametrization is well adapted to our context since it is constructed around a reference point.
Here, we, briefly, recall the construction process of the Darcyan representation.
This parametric representation materialized by coordinates system relatively to a given point on a surface is, in fact, obtained by the superposition of the geodesic level curves around the reference point and the radial lines coming from the same point.
Thus, let S be a two dimensional differential manifold, and let consider U_r the geodesic potential field

coming from a reference point r on S.
This function $U_r : S \rightarrow R^+$ computes for any point p on S the length of the geodesic curve joining it to the reference point r. This function is well defined, since a geodesic curve between two points of a 2D differential manifold exists (Cohen and Kimmel, 1997).
A geodesic level curve of value equal to λ around a reference point r on the surface S can be formulated as follows:

$$L_r^{\lambda} = \{p \in S; U_r(p) = \lambda\} \quad (1)$$

L_r^{λ} is materialized by the set of all points on S having the same geodesic distance λ from r. Therefore, the surface S can be approximately reconstructed by all these geodesic level curves, so that, $S \approx \cup_{\lambda} L_r^{\lambda}$.
We remind as well as the process of radial lines curves construction from a reference point r of the surface S. Like mentioned in (Gadacha and Ghorbel, 2013), the radial curves represent a solution of the following system :

$$\begin{cases} \frac{dP(t)}{dt} = -\nabla U_r(P) \\ P(0) = r \\ \frac{dP(t)}{dt} \mid_{t=0} = \alpha \end{cases} \quad (2)$$

Where $P(t)$ is the geodesic path emanating from r and following the opposite gradient ∇ direction on U_r. Radial lines curves, denoted by C^{α}, are therefore generated according to the angular direction α which can be arbitrary taken. Similar to geodesic level curves, a reconstruction of the surface S can be approximated by $\cup_{\alpha} C^{\alpha}$.
Here we define Darcyan representation D as the superposition of both n geodesic level curves and m radials lines curves relatively to a given point r.

$$D_{k,l}(r) = \left\{ L_r^{\lambda k} \bigcup C_r^{\alpha l}, 1 \leq k \leq n, 1 \leq l \leq m \right\}$$

Figure 2 shows the steps of the Darcyan coordinate system construction.

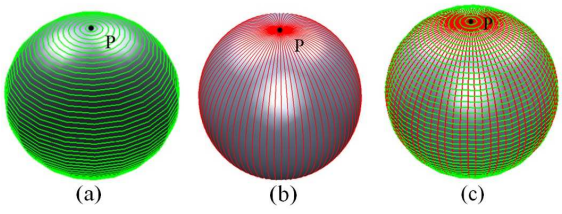

Figure 2: Darcyan system reconstruction: (a)-geodesic level curves, (b)-Radial curves. (c) The superposition of both system of curves.

Consequently, the Darcyan coordinates system is obtained by the superposition of both these sets of curves emanating from a reference point. We propose to extract the intersection points between these two kinds of curves. The resulting discrete parametric points are ordered since each point is indexed by the level of geodesic curve and the radial line it belongs to.

2.3 Principal Curvature Computation

Let S be a given surface. $X : (u,v) \in D \subset R^2 \rightarrow (x(u,v), y(u,v), z(u,v)) \in S \subset R^3$ is a parametric representation of S.
At a point $p = X(x_u, x_v)$ on S, let consider the tangent plane according to the basis (u,v).
The normal vector to S at p is denoted by $N(p) = \frac{x_u \wedge x_v}{\|x_u \wedge x_v\|}$ respecting a chosen orientation.
Thus, the curvature formulation is given using the following coefficients:
$E = x_u.x_u, F = x_u.x_v, G = x_v.x_v, L = x_{uu}.\vec{N}, M = x_{uv}.\vec{N}$ and $N = x_{vv}\vec{N}$

$$K_G = \frac{LN - M^2}{EG - F^2}$$
$$K_M = \frac{EN - 2FM + GL}{2(EG - F^2)}$$

E, F and G denote the first fundamental coefficients, while L, M, N are the second ones.
K_G and K_M represent, respectively, the Gaussian curvature and the Mean curvature $p = X(x_u, x_v)$.
Therefore, the principal curvatures are deducted from these formulations $K_G = k_{max}.K_{min}$ and $K_M = \frac{(k_{max} + k_{min})}{2}$.
k_{max} and k_{min} define the principal maximal and minimal curvatures respectively.

2.4 Darcyan Principal Curvature Fields Descriptor

Relying on the Darcyan representation and the principal curvature fields computation on this local parametrization recalled above, we define a novel 3D shape descriptor, based on intrinsic geometric property, which is invariant under Euclidean motions.

We propose to compute the mean of both principal maximal and minimal curvatures on the intersection points of each geodesic level curve. We denote $\overline{k_{max}^i}$ and $\overline{k_{min}^i}$ the mean of, respectively, k_{max} and k_{min} for the i^{th} geodesic level curve. Hence the novel descriptor is defined by $\left\{ \overline{k_{max}^1}, \overline{k_{min}^1}, .., \overline{k_{max}^i}, \overline{k_{min}^i}, ..., \overline{k_{max}^m}, \overline{k_{min}^m} \right\}_{1 \leq i \leq m}$. Here, m indicates the number of geodesic level curves. The proposed descriptor is illustrated in Figure 3.

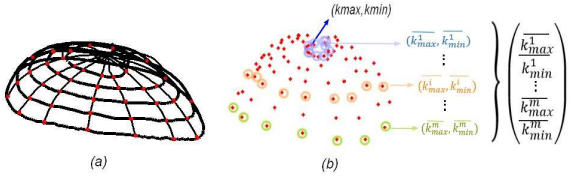

Figure 3: Illustration of the proposed descriptor: (a) the Darcyan representation construction around a reference point, (b) the vector of curvature fiels computation and the obtained intersection points(in red color).

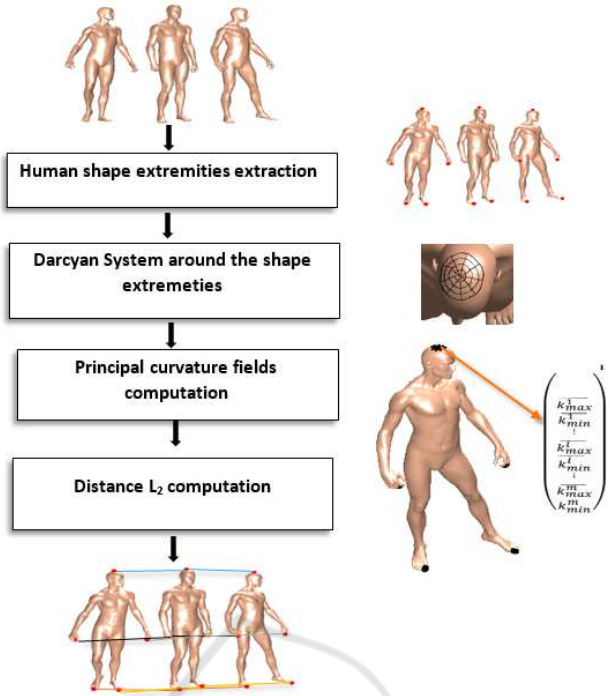

Figure 4: 3D human shapes matching approach.

2.5 3D Human Shapes Extremities Matching

In order to establish non-rigid correspondence between human surface objects, we compute the proposed descriptor around each extreme point. The generated vectors consist on the mean of principal curvature field values over the parametric discrete points. Thereafter, We search for the minimal distance L_2 between all the pairs of the resulting vectors to find the most similar ones.
The targeted matching is then acquired by finding the similarity between the resulting descriptors. This process is also illustrated in Figure 4.

3 EXPERIMENTATION

In this section, we present the experimental results in order to test the effectiveness of our approach. We have conducted the experiments on several 3D human objects in different poses from the TOSCA database (Bronstein and Bronstein, 2008) which contains 3D objects undergoing non-rigid deformations.
We first of all present the approximation of the proposed description steps on the 3D meshes.

3.1 Approximation on 3D Meshes

A 3D object is assumed to be a 2D differential manifold. In practice, it is materialized by a 3D mesh. It is, therefore, necessary to approximate the proposed approach on the 3D meshes. The computation of the geodesic paths and distances on the triangle meshes is achieved by the use of the Fast Marching algorithm (Kimmel and Sethian, 1998). While for the principal curvature computation, we rely on the algorithm of (Meyer et al., 2002). Figure 5 illustrates the Darcyan intrinsic parametric representation around the extremities of a 3D human body mesh.

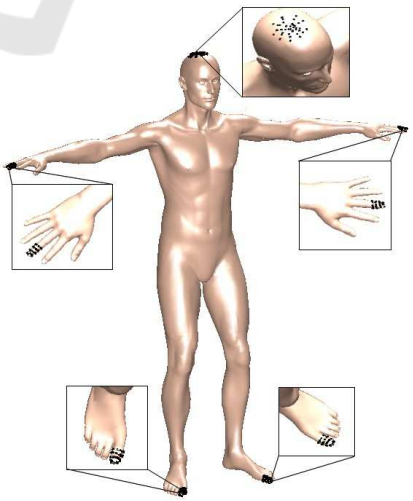

Figure 5: Darcyan representation around a human body extremities from the TOSCA dataset.

3.2 The Correspondence Results

We evaluate our matching approach on different human objects of the TOSCA database (David, Victoria and Michael). We have chosen for each object the same number of poses. After the normalization of these shapes, we have extracted the extremities for all these body shapes. We have, then, constructed our proposed descriptor around these selected points. Figure 6 shows some results of our correspondence method.

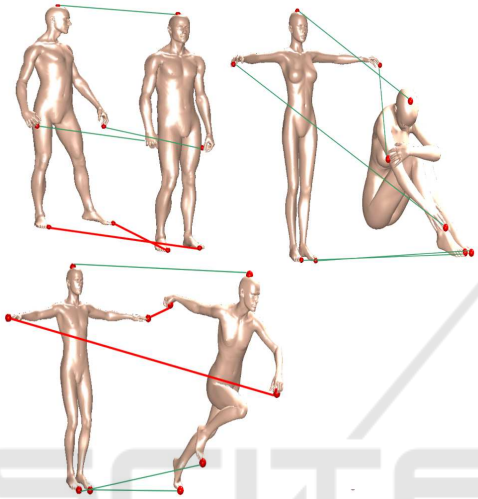

Figure 6: Correspondence results for various human models from the TOSCA dataset, green lines indicate correct matches.

The obtained correct correspondence percentages range from 80% to 100% for the three human models in the chosen poses. The bars colored in blue, in Figure 7, show the correct matching rates. We deem that our approach seems to be able of handling 3D human shapes with various poses.

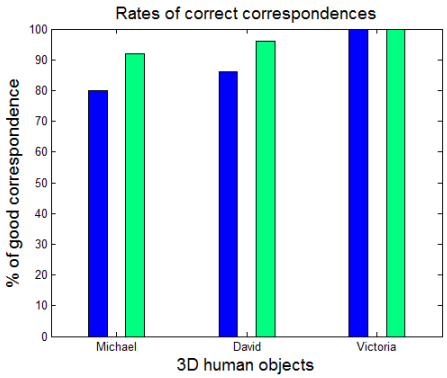

Figure 7: The Correspondence rates for human models from the TOSCA dataset, the blue and green colors indicate, respectevely, the percentage of the correct matches and the obtained ones allevating the problem of the symmetry.

The resulting correspondences show, in some cases, a confusion in the human sides. Hence, a left hand or a left foot may be matched to a right one of another object. This confusion is due to the symmetric structure of the human shape.
To alleviate the problem of the symmetry, we propose to add another geometrical property that could distinguish the right part from the left one of the human body. For this type of shapes, the top of the head is the unique extreme point that has not a symmetrical equivalent.
Thus, we propose to compute the sign of the angle between the two vectors V_1 and V_2: the vector V_1 is a reference one. It corresponds to the tangent to the geodesic curve at the top of the head and joining this point to the tip of the noise. For the vector V_2, it corresponds to the tangent at the top of the head to the geodesic curve joining this last point and the other selected extremities (Figure 8).

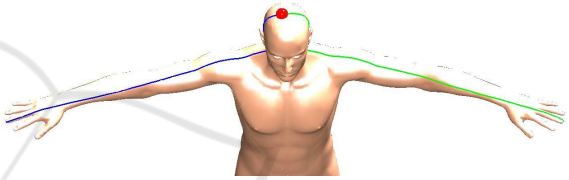

Figure 8: Geodesic curves joining the top of the head and the hand extremities.

The computed angle for the right part of the human body has an opposite sign comparing with the one of the left part. This process allows to raise up the correspondence results as shown in Figure 9. For the object David the percentage of correct correspondence increases from 86% to 96% for the object David and from 80% to 92% for the object Michael. The green bars in Figure 7 show the new percentages.

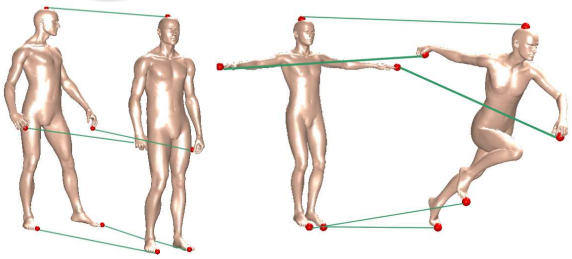

Figure 9: Correspondence after the symmetry correction.

4 CONCLUSIONS

In this paper, we have proposed a novel approach to establish the correspondence between 3D human bodies undergoing non-rigid deformations. We have presented a novel intrinsic description based on a princi-

pal curvatures computation on a local parametrization using the Darcyan coordinates system. We have also proposed a solution for the problem of the symmetrical extremities. The obtained results show the performance of our proposed method for studying the 3D human body matching.

In future works, we intend to achieve the optimal resolution of the local Darcyan representation by finding the suitable number of the geodesic levels and the radial lines curves. We propose also to perform the experimentation on others 3D human databases with different properties and to test the robustness of the intrinsic descriptor to the noise.

REFERENCES

Aalo, Y., Dubrovina, A., and Kimmel, R. (2013). Spectral generalized multi-dimensional scaling. pages 380–392.

Bronstein, A. and Bronstein, M. (2008). Regularized partial matching of rigid shapes. In *European Conference on Computer Vision*, pages 143–154. Springer.

Bronstein, A. M., Bronstein, M. M., and Kimmel, R. (2006). Generalized multidimensional scaling: a framework for isometry-invariant partial surface matching. *Proceedings of the National Academy of Sciences of the United States of America*, 103(5):1168–1172.

Bronstein, A. M., Bronstein, M. M., Kimmel, R., Series, I. M. a. P., Hall, L., and E, C. S. S. (2009). A Gromov-Hausdorff Framework with Diffusion Geometry for Topologically-Robust Non-rigid Shape Matching. pages 612–626.

Cohen, L. and Kimmel, R. (1997). Global Minimum for Active Contour Models. *International Journal on Computer Vision*, 24(1):57–78.

Gadacha, W. and Ghorbel, F. (2013). A stable and accurate multi-reference representation for surfaces of R3: Application to 3D faces description. *IEEE International Conference on Automatic face and Gesture Recognition (FG2013), Shanghai- China*.

Jiang, L., Zhang, X., and Zhang, G. (2013). Partial shape matching of 3D models based on the Laplace-Beltrami operator eigenfunction. *Journal of Multimedia*, 8(6):655–661.

Julien, T., Mohamed, D., and Jean-Philippe, V. (2006). Invariant highlevel reeb graphs of 3d polygonal meshes. *International Symposium on 3D Data Processing, Visualization, and Transmission (3DPVT)*, page 105?112.

Kim, V. G., Lipman, Y., and Funkhouser, T. (2011). Blended intrinsic maps. *ACM Transactions on Graphics*, 30(4):1.

Kimmel, R. and Sethian, J. a. (1998). Computing geodesic paths on manifolds. *Proceedings of the National Academy of Sciences of the United States of America*, 95(15):8431–8435.

Meyer, M., Desbrun, M., Schröder, P., and Barr, A. H. (2002). Discrete Differential-Geometry Operators for Triangulated 2-Manifolds. *International Workshop on Visualization and Mathematics*.

Ovsjanikov, M., Mérigot, Q., Mémoli, F., and Guibas, L. (2010). One point isometric matching with the heat kernel. *Eurographics Symposium on Geometry Processing*, 29(5):1555–1564.

Sun, J., Chen, X., and Funkhouser, T. A. (2010). Fuzzy geodesics and consistent sparse correspondences for: eformable shapes. 29(5):1535–1544.

Taylor, J., Shotton, J., Sharp, T., and Fitzgibbon, A. (2012). The vitruvian manifold: Inferring dense correspondences for one-shot human pose estimation. pages 103–110.

Thompson, D. (1917). *On growth and form*. University press in Cambridge, Cambridge, MA.

Van Kaick, O., Zhang, H., Hamarneh, G., and Cohen-Or, D. (2010). A Survey on Shape Correspondence. *Computer Graphics Forum*, xx:1–23.

Wei, L., Huang, Q., Ceylan, D., Vouga, E., and Li, H. (2015). Dense human body correspondences using convolutional networks. *arXiv preprint arXiv:1511.05904*.

Yaron, L. and Thomas, F. (2009). Möbius voting for surface correspondence. 28(3):72.

Yusuf Sahillioğlu, Y. Y. (2014). Multiple shape correspondence by dynamic programming. 33(7):121–130.

Zhang, H., Sheffer, A., Cohen-Or, D., Zhou, Q., Van Kaick, O., and Tagliasacchi, A. (2008). Deformation-driven shape correspondence. *Eurographics Symposium on Geometry Processing*, 27(5):1431–1439.

Zheng, Y., Tai, C.-L., Zhang, E., and Xu, P. (2013). Pairwise harmonics for shape analysis. *IEEE transactions on visualization and computer graphics*, 19(7):1172–1184.